AAC Accepted Manuscript Posted Online 25 October 2021 Antimicrob Agents Chemother doi:10.1128/AAC.01371-21 Copyright © 2021 American Society for Microbiology. All Rights Reserved.

- 1 Exploration of the Pharmacodynamics for Pseudomonas aeruginosa Biofilm Eradication by
- 2 Tobramycin
- 3
- 4 Devin Sindeldecker^{ab#}, Shaurya Prakash^{cd}, Paul Stoodley^{aef}
- 5

6

USA^a, Biomedical Sciences Graduate Program, The Ohio State University, Columbus, Ohio,
USA^b, Department of Mechanical & Aerospace Engineering, The Ohio State University,
Columbus, Ohio, USA^c, Comprehensive Cancer Center, The Ohio State University, Columbus,
Ohio, USA^d, Department of Orthopaedics, The Ohio State University, Columbus, Ohio, USA^e,
National Center for Advanced Tribology at Southampton (nCATS), Mechanical Engineering,
University of Southampton, Southampton, UK^f.
Running Head: Biofilm Eradication

Department of Microbial Infection and Immunity, The Ohio State University, Columbus, Ohio,

- 14
- 15 [#]Address correspondence to Devin Sindeldecker, Devin.Sindeldecker@osumc.edu.
- 16 Department of Microbial Infection & Immunity,
- 17 The Ohio State University,
- 18 760 BRT, 460 West, 12th Avenue,
- 19 Columbus, OH 43210, USA.
- 20 *E*-mail: Devin.Sindeldecker@osumc.edu
- 21
- 22 Prepared for ASM Antimicrobial Agents and Chemotherapy

Pseudomonas aeruginosa is a Gram-negative, opportunistic pathogen which is involved in 24 25 numerous infections. It is of growing concern within the field of antibiotic resistant and tolerance and often exhibits multi-drug resistance. Previous studies have shown the emergence of antibiotic 26 resistant and tolerant variants within the zone of clearance of a biofilm lawn after exposure to 27 28 aminoglycosides. As concerning as the tolerant variant emergence is, there was also a zone of 29 killing (ZOK) immediately surrounding the antibiotic source from which no detectable bacteria emerged or were cultured. In this study, the ZOK was analyzed using both in vitro and in silico 30 methods to determine if there was a consistent antibiotic concentration versus time constraint (area 31 32 under the curve, (AUC)) which is able to completely kill all bacteria in the lawn biofilms in our in vitro model. Our studies revealed that by achieving an average AUC of 4,372.5 µg*hr/mL, 33 complete eradication of biofilms grown on both agar and hydroxyapatite was possible. These 34 35 findings show that appropriate antibiotic concentrations and treatment duration may be able to treat antibiotic resistant and tolerant biofilm infections. 36

37

38 Introduction

Pseudomonas aeruginosa is a Gram-negative bacterium and opportunistic pathogen. Most 39 commonly, it is associated with cystic fibrosis (CF) related lung infections but is also implicated 40 in chronic wounds and post-surgical site infections (1-3). Antimicrobial tolerance and resistance 41 42 are also major concerns with *P. aeruginosa*, as the formation of biofilms, variant populations, and 43 multidrug resistance mechanisms are also prevalent (4-8). A recent study on the antibiotic 44 resistance rates of *P. aeruginosa* have shown a minimum 20% rate of resistance for carbapenems, cephalosporins, aminoglycosides, and piperacillin/tazobactam (9). In addition, multi-drug 45 resistance was also found in 20% of infections (9). 46

47

In a previous study, variant colony phenotypes of P. aeruginosa emerging within the region 48 cleared by a tobramycin-loaded calcium sulfate bead were identified (8). This region of bacterial 49 50 lawn clearance is referred to as the zone of clearance (ZOC, Figure 1). These variant colonies included classical resistance, persister cells, viable but non-culturable like colonies (VBNC-like), 51 52 and newly identified, tolerant, phoenix colonies (8). While the significance of these emergent phenotypes may be of concern from a clinical standpoint, it is important to note that there was also 53 a smaller, consistent region within the ZOC, immediately adjacent to the antibiotic source, from 54 which no variants emerged or were cultured (8, 14). This previously reported zone, referred to as 55 56 the zone of killing (ZOK), represents a region of complete biofilm killing including antibiotic tolerant and resistant variants (Figure 1, (8, 14)). 57

58

59 INSERT FIGURE 1 HERE

60

Antimicrobial Agents and

Chemotherapy

61

antibiotics (15, 16), further research into the pharmacodynamics necessary to eliminate biofilms is 62 needed. Currently, the primary method for measuring pharmacokinetics and pharmacodynamics 63 (PK/PD) in vitro is the modified Calgary biofilm device method (17). This method is used to grow 64 65 biofilms on pegs which are suspended in wells of a 96-well plate before exposing the biofilms to antibiotics (17). Use of this method can be complicated by contamination risks, variation in 66 67 recovered biofilm after antibiotic exposure due to the rinsing steps necessary, and residual antibiotics left after rinses (17). In this study, the ZOK from which no bacteria could be cultured 68 was further analyzed using a new method for exploring PK/PD in vitro. We hypothesized that the 69 70 junction between the outer edge of the ZOK and the region containing the emergent variants represents an antibiotic concentration versus treatment time constraint in which complete bacterial 71 72 biofilm eradication can be achieved. In order to evaluate our hypothesis, a combination of a biofilm 73 plate in vitro model and an in silico approach was used to identify the concentration and time 74 (AUC) necessary to eliminate a *P. aeruginosa* biofilm, including variants which can typically 75 survive antibiotic therapy, using tobramycin. Additionally, substrates using both a tissue mimic 76 (agar, (18, 19)) and a bone mimic (hydroxyapatite (HA), (20)) were used to determine if the biofilm 77 substrate would affect the ability of an AUC to completely eradicate the biofilm.

While pharmacodynamic studies have been done using planktonic P. aeruginosa exposed to

78

79 Results

Zones of Clearance of Biofilms Exhibit Dose-dependency 80

In order to begin assessing the possible correlation between the ZOK and an antibiotic 81 82 concentration versus time constraint, twenty-four hour biofilm lawns of P. aeruginosa Xen41 were generated as reported previously (8, 18) before being exposed to various weight quantities of 83

84 tobramycin (Figure 2). In vitro Imaging System (IVIS) evaluation of the biofilm lawns post tobramycin exposure showed the emergence of dose-dependent ZOCs which continued to expand 85 over time. Within the ZOC, variant colonies began to emerge and encroach on the ZOC which had 86 formed. However, there was also a dose-dependent ZOK within the ZOC from which no 87 88 discernable bacterial activity was detected (Figure 2). It should also be noted that the luminescence 89 which appears to overly the antibiotic disks is likely due to surface associated biofilm growth. The 90 presence of the disk likely provides an additional substrate for biofilm growth and allows for initial levels of high bioluminescence before the tobramycin ultimately is able to clear the formed 91 92 biofilm.

93

INSERT FIGURE 2 HERE 94

95

Profiling of the ZOK Confirms Dose-dependency 96

After exposure of the biofilm lawns to tobramycin, the plates were further analyzed to obtain 97 98 measurements of the ZOK over time. These measurements were used to generate plots (Figure 3) which show the linear generation of the ZOC, followed by a ZOC peak right before variant 99 colonies began to emerge. The peak of the plot for each weight quantity of tobramycin shifts to a 100 later time point as the weight quantity increases. This is likely due to the time necessary for the 101 102 antibiotic to diffuse to low enough concentrations to allow variant colonies to begin to emerge. As 103 variant colonies began to emerge and grow within the ZOC, this allows the ZOK to be visualized. 104 The plots then plateaued as the ZOK became more apparent in which no detectable bacteria emerged or grew. Once the ZOK stabilized, the radius of the edge of the ZOK was noted, as this 105

5

Antimicrobial Agents and

Chemotherapy

106 is the point likely to represent the minimum antibiotic concentration away from the antibiotic 107 source versus time constraint necessary for complete biofilm eradication including the killing of 108 any antibiotic tolerant or resistant variants. These radii values and time points were then used to generate antibiotic diffusion plots using numerical modeling. In addition, a time-kill curve was 109 generated for the ZOK of a 1 mg tobramycin loaded disk. At 40 hours post tobramycin exposure, 110 111 a slight decrease in CFUs/cm² can be seen which further decreases and becomes significant (p=0.017) by 48 hours. At 72 hours of tobramycin exposure and thereafter, no CFUs are able to be 112 recovered from within the ZOK (Figure 4). 113

114

115 **INSERT FIGURE 3 HERE**

116

INSERT FIGURE 4 HERE 117

118

119 Computational Modeling Identified an Area Under the Curve Value for Biofilm Eradication

120 Using the data collected from the profiling of the ZOC and ZOK, a model was used (21) to predict the tobramycin concentration over time at the ZOK radius identified for each mass of tobramycin 121 122 used (Figure 5). The model calculates the concentration of tobramycin over time assuming Fickian 123 diffusion in a finite space (21, 22). The plots in Figure 3 show a dose-dependent increase in the 124 antibiotic concentration after antibiotic placement until concentrations for each weight quantity of antibiotic peaked (120.9, 241.9, 483.8, and 967.5 µg/mL, respectively). The concentration then 125 gradually begins to decrease and plateau as the system continues to approach equilibrium (12.5, 126 127 25, 50, 100 mg/mL, respectively) for each weight quantity (250, 500, 1000, 2000 µg, respectively). 128 An AUC (µg*hr/mL) was calculated for each plot to determine the necessary minimum value

129 necessary for ZOK generation for each of the amounts of tobramycin (Table 1). Interestingly, 130 despite a 4-fold change in the starting tobramycin weight quantity, the AUCs for each were 131 relatively similar. This observation highlights the importance of an AUC being taken into 132 consideration during antibiotic dosing as opposed to purely relying on the antibiotic concentration 133 alone. The mean of the AUC values was also calculated to determine that the average minimum 134 value necessary for biofilm eradication, including antibiotic tolerant and resistant variants, was 135 approximately $4,372.5 \ \mu g^{*}hr/mL$. The concentration of antibiotic needed here is much higher than standard minimum inhibitory concentrations (MIC) for tobramycin and P. aeruginosa PAO1 (4 136 μ g/mL). Additionally, by dividing the AUC by the MIC, an AUC/MIC ratio of 46 can be calculated 137 138 when normalizing for 24 hours. This higher concentration ratio is likely responsible for the ability to kill even antibiotic resistant and tolerant variants. 139

140

141 INSERT FIGURE 5 HERE

142

143 INSERT TABLE 1 HERE

144

145 Identified AUC Can Eradicate Biofilms Grown on an Alternate Substrate

146 In order to test the AUC value associated with complete *P. aeruginosa* biofilm eradication by 147 tobramycin, biofilms were grown on LB agar coated pegs, as well as HA coupons and plastic pegs 148 as alternate biofilm substrates. Biofilm colony forming units (CFUs) were measured for biofilms 149 exposed to tobramycin at the approximate 4,372.5 μ g*hr/mL AUC. LB agar coated peg, HA 150 coupon, and plastic peg biofilms were exposed to tobramycin for 24 hours at a stable concentration 151 of 182 μ g/mL (Figure 6) which equals an approximate AUC value of 4372.5 μ g*hr/mL. In all Antimicrobial Agents and

Chemotherapy

tobramycin exposure samples, no CFUs were recovered, indicating a complete eradication of the biofilms. Additionally, a control was run at a 0.1 AUC equivalent on agar grown biofilms. The control samples showed full lawns of growth after tobramycin treatment, indicating minimal effectiveness of biofilm clearance. These results confirm that by obtaining a high concentration of antibiotics for at least 24 hours, complete eradication of a *P. aeruginosa* lawn biofilm including any antibiotic resistant or tolerant variants was possible and, substrate differences were not relevant.

159

160 INSERT FIGURE 6 HERE

161

162 Discussion

163 P. aeruginosa is an opportunistic, bacterial pathogen which has been associated with numerous 164 infection sites. It has also been shown to readily develop tolerance and resistance to multiple 165 antibacterial drugs leading to an increased concern for complicated and difficult to treat infections 166 (23-25). Previously, the antibiotic tolerant phoenix and the VBNC-like phenotypes were identified, in addition to classically resistant colonies and persister cells, within the ZOC of produced by 167 168 antibiotics released from tobramycin loaded Kirby-Bauer filter disks and CaSO4 beads (8). While 169 the emergence of these variant colonies is concerning, it was also shown that there was a consistent 170 ZOK immediately adjacent to the antibiotic source from which no bacteria emerged or were cultured. Replica plating was also performed on these plates and showed no growth within the 171 ZOK, indicating that this region is sterile (8). In these studies, both the ZOC and ZOK were 172 173 measured since it is not possible to differentiate between the two zones at early time points before 174 variant colonies begin to emerge. The distinct ZOK within the ZOC indicates a smaller region

AAC

where we may be able to eliminate antibiotic resistance and tolerance with high enough concentrations of antibiotics over extended time frames. By understanding how antibiotic kinetics effect biofilms and antibiotic resistant and tolerant variants, we will be better prepared to control and prevent the rise of these dangerous biofilm infections.

179 In this study, the ZOK of *P. aeruginosa* biofilms was analyzed to determine the antibiotic 180 pharmacodynamics necessary for its generation. For our study, a combination of a biofilm plate 181 model and numerical modeling was used as a simpler alternative to the modified Calgary biofilm 182 plate model (17). The methods presented here could be adapted for further in vitro biofilm PK/PD studies including the use of other bacterial species and antibiotics. Previous studies have shown 183 184 the importance of not only the concentration of antibiotic used but also the exposure time of the 185 biofilm-growing bacteria to the antibiotic. These studies on the antibiotic AUC have shown that as exposure time increases, the minimum concentration needed for biofilm eradication (MBEC) 186 decreases (26). In addition, pharmacodynamic studies on the efficacy of antibiotics against bacteria 187 188 have shown an importance in the ratio of AUC/MIC (27, 28). The AUC/MIC ratio necessary for 189 bactericidal activity against P. aeruginosa by tobramycin has been shown to be approximately 42. 190 For our studies, various weight quantities of tobramycin were used which allowed for a more complete understanding of these required pharmacodynamics. While the varying masses of 191 192 antibiotic used showed large, dose-dependent variations in the ZOK diameters, it was interesting 193 that the AUCs calculated for each mass did not scale similar to the weight of the antibiotic, ranging 194 from 3560-4870 µg*hr/mL, although there was a nearly 8-fold increase in antibiotic dosing (250-195 2000 μ g). At an approximate AUC of 4372.5 μ g*hr/mL and an MIC of 4 μ g/mL, the AUC/MIC ratio for biofilm eradication by tobramycin would be approximately 46 when normalized for a 24-196 197 hour timeframe. Previous studies on local tobramycin concentrations achieved when treating

198 orthopedic infections with tobramycin loaded methylmethacrylate bone cement has shown that the 199 concentrations peak at approximately 40 µg/mL around 1 hour after beginning exposure. The 200 concentration then drops to approximately 20 µg/mL through 24 hours (30). These lower 201 concentrations may explain the prevalence of post-surgical infection treatment failure, as antibiotic 202 tolerant or resistant variants may be able to survive. In addition, while C_{max}/MIC is the metric 203 typically used in relation to tobramycin (27), it has been shown that by using AUC/MIC, better 204 clinical outcomes are able to be achieved (28). This may be especially true when treating biofilm 205 infections as biofilms are inherently more tolerant of antibiotics due to slow diffusion of the 206 antibiotic into the biofilm matrix as well as heterogeneity in the biofilm metabolism (31), 207 increasing the importance of time-dependence. Our observations suggest that a minimum AUC representing the total treatment effect (concentration x time) may be used to facilitate the complete 208 209 eradication of P. aeruginosa biofilms, including variants that without this treatment could re-seed 210 infection (32). It is also important to note that although VBNC-like colonies may be present in our 211 systems, they would not be apparent as they are unable to be cultured by nature. However, this 212 characteristic also would likely prevent re-emergence in a clinical environment.

213 In addition to using different weight quantities of tobramycin, different substrates were also used 214 to provide breadth to the relevance of the identified 4,372.5 µg*hr/mL necessary for biofilm 215 eradication. It is possible that biofilms grown on different substrates could have differing phenotypes, including variations in metabolic pathways which may play a role in the efficacy of 216 217 antibiotics (33, 34). Although biofilm phenotypic variations can occur, the identified AUC was 218 able to eradicate biofilms grown on both a tissue mimic such as agar (18, 19) and a material 219 commonly known to be important for bone infections (HA, (20)), indicating that the use of the 220 AUC metric for biofilm treatment is independent of the substrate rigidity and providing relevance

10

Antimicrobial Agents and

Chemotherapy

221 to other fields such as dentistry and orthopedics. The observation evaluating the clearance of 222 biofilms from two distinct substrates is important clinically as biofilms are able to grow in the 223 human body on soft tissues such as lung tissue or skin and on hard substrates such as bone or implanted devices (20, 35, 36). Clearly, optimizing the AUC as a treatment effect metric needs 224 further work, but the values reported here provide a specific evaluation for tobramycin and P. 225 226 aeruginosa. Therefore, further research, including studies involving other antibiotic classes and 227 bacterial species, is needed for a more complete understanding of the ability to eradicate bacterial 228 biofilm infections.

229

230 Methods and Methods

231 Bacterial strains and culture conditions

The metabolically driven, bioluminescent strain P. aeruginosa Xen41 (Xenogen Corp., USA) was 232 used for the imaging portion of this study. Additionally, P. aeruginosa PAO1 (15) which is both 233 234 a standard lab strain and the parent strain for P. aeruginosa Xen41 was used in this study. Culture plates were prepared by from glycerol stock cultures stored at -80°C using 100 mm petri plates 235 236 (Fisher Scientific, USA) containing 20 mL of Luria-Bertani (LB) agar. Streaked plates were incubated at 37°C for 24 hours to allow for individual colonies to grow. Individual colonies were 237 examined for proper morphology and then isolated and transferred to 20 mL of LB broth. Broth 238 239 cultures were incubated overnight in a shaking incubator set to 37°C and 200 rpm.

240

241 Generation of Biofilm Lawns

Overnight broth cultures of *P. aeruginosa* Xen41 were diluted to an OD₆₀₀ of 0.1 in LB broth and 100 µL aliquots were spread onto plates containing 20 mL of sterile, LB agar. These plates were incubated at 37°C with 5% CO₂ for 24 hours to allow for biofilm lawns to generate. Lawn generation was confirmed both visually and by using *in vitro* imaging system (IVIS) imaging.

246

247 Bioluminescence Imaging

Bioluminescence imaging was completed using thirty second exposures in an IVIS system. A
pseudo-color heatmap was overlaid to aid in visualization of the metabolic activity of the biofilms.
The scale for the heatmap is as follows: red indicates high levels of metabolic activity, blue
indicates low levels of metabolic activity, and black indicates no metabolic activity.

252

253 *Exposure of Biofilm Lawns to Antibiotic*

254 After lawn generation, the biofilms were exposed to set masses of tobramycin (250 μ g, 500 μ g, 255 1000 µg, and 2000 µg). Briefly, a 100 mg/mL stock solution of tobramycin was created using 256 tobramycin powder (TCI America, USA) and sterile water. This solution was then used to create 257 dilutions for the other necessary masses of tobramycin. A sterile, filter paper disk was placed in 258 the center of each of the lawn biofilms and then 20 μ L of the appropriate tobramycin solution was 259 placed on the disk to allow for exposure of the biofilm lawns to the desired masses of tobramycin. 260 After antibiotic placement, the plates continued to be incubated at 37°C with 5% CO₂ for five 261 additional days. IVIS images were taken and the zones of killing measured daily.

262

263 Time-kill Curve Generation

In order to measure the CFUs within the ZOK over time, time-kill curves were generated.
Biofilm lawns were generated as above and were either exposed to 1 mg of tobramycin on a
filter paper disk or not exposed for controls. At various time points, a 1 cm x 1 cm area of
biofilm lawn, located between 1 and 2 cm from the disk, was scraped using a sterile loop and
placed into 1 mL of sterile PBS. A dilution series was then made and plated. CFUs were counted
for each sample and curves were generated.

270

271 Computational Modeling

In order to calculate the antibiotic concentration versus time necessary for development of the ZOK, an analytical solution was used to estimate the tobramycin concentration, c(r, t) for a 120 hour treatment time. The solution for the diffusion of antibiotic bead or disk in an agar plate is given by:

276
$$c(r, t) = \frac{m}{h_0} \frac{1}{4\pi D(t+t_0)} \exp\left(-\frac{r^2}{4D(t+t_0)}\right)$$

where the diffusion coefficient of tobramycin in agar is D and was experimentally determined to 277 be 3.84×10^{-10} m²/s, *m* is the mass of antibiotic added to the source, h_0 is the height of the agar, 278 and r is the position coordinate relative to the center of a paper disk (19, 21, 22, 37). The model 279 assumes that antibiotic source is finite with a radius, $r_o = 3$ mm. The model assumed that the inner 280 radius of the petri dish, 70 mm (inner diameter is 140 mm), was >10 times the radius of the paper 281 282 disks (3 mm) used, whereas the depth of agar layer was ~3.6 mm. After model generation, an area 283 under the curve (AUC) value was calculated in MATLAB for each curve using the trapezoidal rule function, and the mean of the AUCs was also calculated. 284

306

285

286 Testing of AUC on Hydroxyapatite

287 In order to assess whether the AUC required for P. aeruginosa biofilm eradication could be 288 translated to biofilms grown on alternative surfaces, biofilms of P. aeruginosa PAO1 were grown 289 on 0.5 inch hydroxyapatite (HA) coupons (Biosurface Technologies, USA). Overnight LB broth 290 cultures of P. aeruginosa PAO1 were prepared as above. Overnight cultures were diluted to an 291 OD₆₀₀ of 0.1 in LB broth. HA coupons were added to the wells of a 12 well plate before 3 mL of 292 the diluted overnight culture were also added to the wells. The well plate was incubated at 37°C 293 with 5% CO₂ for 24 hours to allow biofilms to form on the HA coupons. Three coupons were then 294 exposed to tobramycin, and three coupons were exposed to PBS only as a control. Briefly, the 295 coupons were removed from the well plate and rinsed in PBS to remove any planktonic bacteria. 296 The coupons were then placed in a fresh 12 well plate for exposure to tobramycin or PBS only. 297 Three mL of a tobramycin solution was used for antibiotic exposure of the coupons for 24 hours 298 at a concentration of 182 µg/mL in order to equal the mean AUC value of 4,368 µg*hr/mL. During 299 the tobramycin exposure, the coupons continued to be incubated at 37°C with 5% CO₂. After 24 300 hours, coupons were removed from the well plate to obtain CFU counts. The coupons were rinsed 301 in PBS before being placed into wells of a fresh 12 well plate containing 3 mL of PBS. This plate 302 was then placed into a water bath sonicator and sonicated for 30 minutes. After sonication, the 303 PBS was removed from each well and centrifuged in order to pellet the bacteria. The pellet was 304 then resuspended in 200 μ L of LB broth and a dilution series was created. The dilution series was 305 plated on 20 mL of LB agar and CFU counts were obtained.

14

307 Testing of AUC on Plastic and Agar

308 In addition to AUC validation on HA coupons, the AUC was also validated on plastic pegs of an MBEC assay biofilm inoculator plate (Innovotech, Canada) as well as MBEC assay biofilm 309 inoculator plate pegs coated in LB agar. Briefly, LB agar coated pegs were prepared as follows. 310 311 $200 \,\mu\text{L}$ of molten LB agar was placed into the wells of a 96 well plate. The MBEC plate, which had previously been cooled to -80° C, was then placed onto the 96 well plate to allow the pegs to 312 dip into the molten LB agar. After 3 seconds, the plate was removed and the agar was allowed to 313 314 finish cooling in a coating on the pegs. After LB agar coating, both LB agar coated pegs and uncoated pegs were exposed to P. aeruginosa PAO1 to allow biofilms to form. An overnight 315 culture of PAO1 was diluted in LB broth at a ratio of 1:1000. 150 µL of the diluted culture was 316 added to wells of 96 well plates. MBEC plates both coated in LB agar and uncoated were placed 317 318 onto the 96 well plates with diluted culture. These plates were then incubated at 37°C with 110 rpm shaking for 24 hours to allow biofilms to develop. After incubation, the pegs were rinsed in 319 320 200 μ L of PBS for 10 seconds. After rinsing, the MBEC plates were placed on 96 well plates 321 containing either 200 µL of 182 µg/mL tobramycin or 200 µL of PBS as a control. These plates 322 were then incubated for an additional 24 hours at 37°C with 110 rpm shaking. After incubation, the MBEC plates were rinsed in wells containing 200 µL PBS and then placed on a fresh 96 well 323 plate with wells containing 200 µL PBS. These plates were then sonicated in a water bath sonicator 324 325 for 30 minutes. After sonication, the bacteria containing PBS was removed and plated in a dilution 326 series. CFU counts were obtained for each sample.

327

328 *Statistical analysis*

- 329 All experiments were replicated in triplicate. ANOVA analysis was completed by GraphPad Prism
- 330 (v8.2.1) with a p-value of 0.05 being considered significant.
- 331

332 Acknowledgements

- 333 This work was supported in part by the Ohio State University College of Medicine and R01
- NIH- GM124436 (PS). We also acknowledge partial support from the National Heart, Lung, and
- Blood Institute (R01HL141941; SP).
- 336 Conflict of interest None declared.

337

338 Figure Legends

339

340 Figure 1 – Emergence of ZOC and ZOK. IVIS images of a representative P. aeruginosa Xen41 plate showing ZOC emergence after exposure to tobramycin. A biofilm lawn was grown for 24 341 342 hours before being exposed to tobramycin on Day 0. Over time, a ZOC (yellow dotted circle) can 343 be seen as the antibiotic clears the background lawn. On Day 4, variant colonies begin to grow 344 within the ZOC and a ZOK (red dotted circle) becomes apparent. The ZOK is the region in which 345 there are no variant colonies or other discernable bacterial activity. In the images, red indicates 346 high levels of metabolic activity, blue indicates low levels of metabolic activity, and black 347 indicates no metabolic activity.

348

Figure 2 – IVIS Imaging of *P. aeruginosa* Biofilms Exposed to Tobramycin. Biofilm lawns of *P. aeruginosa* Xen41 were generated on agar before being exposed to various amounts of tobramycin for a total of five days. Zones of clearance (ZOC) can be seen growing over time for each mass of tobramycin. Although variant colonies emerge from the ZOC, there is a distinct region within the ZOC, marked explicitly in Figure 1, known as the zone of killing (ZOK). In the images, red indicates high levels of metabolic activity, blue indicates low levels of metabolic activity, and black indicates no metabolic activity.

356

Figure 3 – ZOK Expansion Curves for Tobramycin. The ZOK of the plates from Figure 2 were measured over time. The zones follow linearly until the peak (indicated by black arrows), which occurs as variant colonies begin to emerge within the ZOC, and the diameter of the ZOK becomes evident. As these variant colonies continue to emerge and begin to grow, the ZOK reduces. After the peak, the ZOK continues to become more apparent as the area lacking emergence of variant

17

colonies. The ZOK decrease continues as variant colonies emerge until the plot begins to plateau, at which point the ZOK was stable. Data are reported as mean \pm SD (n=3). *p<0.05, **p<0.01.

364

Figure 4 – Time-kill Curve for the ZOK. CFUs within the ZOK of 1 mg of tobramycin were measured over time. Controls CFUs were measured for plates without tobramycin exposure. At 48 hours post tobramycin exposure, a decrease in CFUs begins to be seen, and by 72 hours post tobramycin exposure, no CFUs were able to be recovered from within the ZOK. Data are reported as mean±SD. *p<0.05, ***p<0.001, ****p<0.0001, n=3.

370

Figure 5 – Computational Modeling of Antibiotic Diffusion. The diffusion model shows the spread
of tobramycin over time. The radii used to determine the zones of killing for each antibiotic
quantity was experimentally measured (Figure 2) and used as an input to the model for the
computation of the concentration. All plots show an increase in tobramycin concentration followed
by a decrease following the Fickian diffusion model.

376

Table 1 – AUC Values Associated with Complete Biofilm Eradication in Our Agar Plate Biofilm Model. Values for the AUC (μ g*hr/mL) for each mass of tobramycin were calculated from the plots of Figure 4. The mean of each of these values was also calculated and likely represents the minimum AUC necessary for complete eradication of biofilms, including antibiotic resistant and tolerant variants.

		250 µg	500 µg	1000 µg	2000 µg	Average
A	UC	3560 µg*hr/mL	4730 µg*hr/mL	4330 µg*hr/mL	4870 µg*hr/mL	4372.5 µg*hr/mL

382

383

18

385	P. aeruginosa PAO1 biofilms grown on plastic pegs, LB agar coated pegs, and hydroxyapatite
386	coupons were exposed to 182 $\mu\text{g/mL}$ of tobramycin for 24 hours, equaling an AUC value of
387	approximately 4372.5 µg*hr/mL. Complete biofilm eradication was seen in all of the tobramycin
388	treated samples. ****p<0.0001, n=3.

384

Figure 6 - Eradication of P. aeruginosa Biofilms Grown on Plastic, LB Agar, and Hydroxyapatite.

390 References

391	1.	Hoiby N, Ciofu O, Bjarnsholt T. 2010. Pseudomonas aeruginosa biofilms in cystic fibrosis.
392		Future Microbiol 5:1663-74.
393	2.	Serra R, Grande R, Butrico L, Rossi A, Settimio UF, Caroleo B, Amato B, Gallelli L, de

- Franciscis S. 2015. Chronic wound infections: the role of Pseudomonas aeruginosa and
 Staphylococcus aureus. Expert Rev Anti Infect Ther 13:605-13.
- Shah NB, Osmon DR, Steckelberg JM, Sierra RJ, Walker RC, Tande AJ, Berbari EF. 2016.
 Pseudomonas Prosthetic Joint Infections: A Review of 102 Episodes. J Bone Jt Infect 1:25-30.
- 4. Lewis K. 2010. Persister cells. Annu Rev Microbiol 64:357-72.
- Lewis K. 2008. Multidrug tolerance of biofilms and persister cells. Curr Top Microbiol
 Immunol 322:107-31.
- 402 6. Hall-Stoodley L, Stoodley P. 2005. Biofilm formation and dispersal and the transmission
 403 of human pathogens. Trends Microbiol 13:7-10.
- Zavascki AP, Carvalhaes CG, Picao RC, Gales AC. 2010. Multidrug-resistant
 Pseudomonas aeruginosa and Acinetobacter baumannii: resistance mechanisms and
 implications for therapy. Expert Rev Anti Infect Ther 8:71-93.
- Sindeldecker D, Moore K, Li A, Wozniak DJ, Anderson M, Dusane DH, Stoodley P. 2020.
 Novel Aminoglycoside-Tolerant Phoenix Colony Variants of Pseudomonas aeruginosa.
 Antimicrob Agents Chemother 64.
- 410 9. Appaneal HJ, Caffrey AR, Jiang L, Dosa D, Mermel LA, LaPlante KL. 2018. Antibiotic
 411 resistance rates for Pseudomonas aeruginosa clinical respiratory and bloodstream isolates
 412 among the Veterans Affairs Healthcare System from 2009 to 2013. Diagn Microbiol Infect
 413 Dis 90:311-315.
- 414 10. Brauner A, Fridman O, Gefen O, Balaban NQ. 2016. Distinguishing between resistance,
 415 tolerance and persistence to antibiotic treatment. Nat Rev Microbiol 14:320-30.
- 416 11. Jana S, Deb JK. 2006. Molecular understanding of aminoglycoside action and resistance.
 417 Appl Microbiol Biotechnol 70:140-50.
- 418 12. Lewis K. 2007. Persister cells, dormancy and infectious disease. Nat Rev Microbiol 5:48419 56.

Antimicrobial Agents and

Antimicrobial Agents and

Chemotherapy

Mulcahy LR, Burns JL, Lory S, Lewis K. 2010. Emergence of Pseudomonas aeruginosa
strains producing high levels of persister cells in patients with cystic fibrosis. J Bacteriol
192:6191-9.

14. Devendra H. Dusane JRB, Devin Sindeldecker, Casey W. Peters, Anthony Li, Nicholas R.
Farrar, Scott M. Diamond, Cory S. Knecht, Roger D. Plaut, Craig Delury, Sean S. Aiken,
Phillip A. Laycock, Anne Sullivan, Jeffrey F. Granger, and Paul Stoodley. 2019. Complete
Killing of Agar Lawn Biofilms by Systematic Spacing of Antibiotic-Loaded Calcium
Sulfate Beads. Materials.

MacGowan AP, Wootton M, Holt HA. 1999. The antibacterial efficacy of levofloxacin and
ciprofloxacin against Pseudomonas aeruginosa assessed by combining antibiotic exposure
and bacterial susceptibility. J Antimicrob Chemother 43:345-9.

Madaras-Kelly KJ, Ostergaard BE, Hovde LB, Rotschafer JC. 1996. Twenty-four-hour
area under the concentration-time curve/MIC ratio as a generic predictor of
fluoroquinolone antimicrobial effect by using three strains of Pseudomonas aeruginosa and
an in vitro pharmacodynamic model. Antimicrob Agents Chemother 40:627-32.

- Hengzhuang W, Hoiby N, Ciofu O. 2014. Pharmacokinetics and pharmacodynamics of
 antibiotics in biofilm infections of Pseudomonas aeruginosa in vitro and in vivo. Methods
 Mol Biol 1147:239-54.
- 438 18. Dusane DH, Lochab V, Jones T, Peters CW, Sindeldecker D, Das A, Roy S, Sen CK,
 439 Subramaniam VV, Wozniak DJ, Prakash S, Stoodley P. 2019. Electroceutical Treatment
 440 of Pseudomonas aeruginosa Biofilms. Sci Rep 9:2008.
- Lochab V, Jones TH, Dusane DH, Peters CW, Stoodley P, Wozniak DJ, Subramaniam VV,
 Prakash S. 2020. Ultrastructure imaging of Pseudomonas aeruginosa lawn biofilms and
 eradication of the tobramycin-resistant variants under in vitro electroceutical treatment. Sci
 Rep 10:9879.
- 445 20. Moley JP, McGrath MS, Granger JF, Stoodley P, Dusane DH. 2018. Reduction in
 446 Pseudomonas aeruginosa and Staphylococcus aureus biofilms from implant materials in a
 447 diffusion dominated environment. J Orthop Res 36:3081-3085.
- 448 21. Hoiby N, Henneberg KA, Wang H, Stavnsbjerg C, Bjarnsholt T, Ciofu O, Johansen UR,
 449 Sams T. 2019. Formation of Pseudomonas aeruginosa inhibition zone during tobramycin

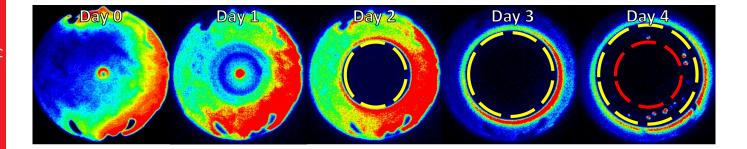
21

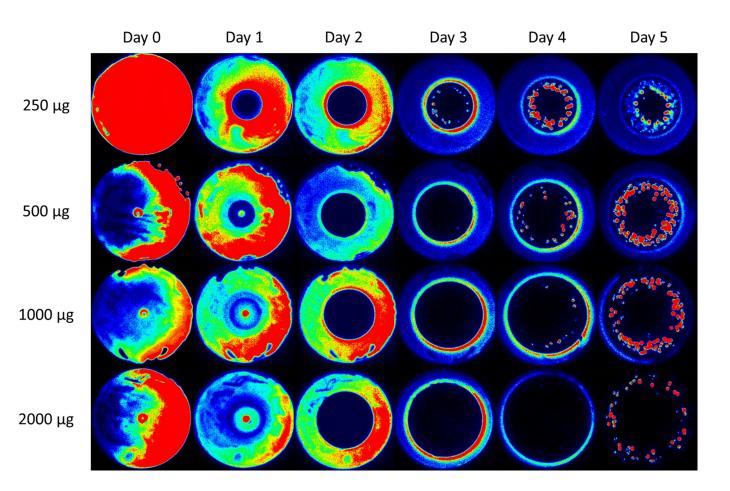
450		disk diffusion is due to transition from planktonic to biofilm mode of growth. Int J
451		Antimicrob Agents 53:564-573.
452	22.	Gefen O, Chekol B, Strahilevitz J, Balaban NQ. 2017. TDtest: easy detection of bacterial
453		tolerance and persistence in clinical isolates by a modified disk-diffusion assay. Sci Rep
454		7:41284.
455	23.	Pang Z, Raudonis R, Glick BR, Lin TJ, Cheng Z. 2019. Antibiotic resistance in
456		Pseudomonas aeruginosa: mechanisms and alternative therapeutic strategies. Biotechnol
457		Adv 37:177-192.
458	24.	Pachori P, Gothalwal R, Gandhi P. 2019. Emergence of antibiotic resistance Pseudomonas
459		aeruginosa in intensive care unit; a critical review. Genes Dis 6:109-119.
460	25.	Ciofu O, Tolker-Nielsen T. 2019. Tolerance and Resistance of Pseudomonas aeruginosa
461		Biofilms to Antimicrobial Agents-How P. aeruginosa Can Escape Antibiotics. Front
462		Microbiol 10:913.
463	26.	Castaneda P, McLaren A, Tavaziva G, Overstreet D. 2016. Biofilm Antimicrobial
464		Susceptibility Increases With Antimicrobial Exposure Time. Clin Orthop Relat Res
465		474:1659-64.
466	27.	Burkhardt O, Lehmann C, Madabushi R, Kumar V, Derendorf H, Welte T. 2006. Once-
467		daily tobramycin in cystic fibrosis: better for clinical outcome than thrice-daily tobramycin
468		but more resistance development? J Antimicrob Chemother 58:822-9.
469	28.	Smith PF, Ballow CH, Booker BM, Forrest A, Schentag JJ. 2001. Pharmacokinetics and
470		pharmacodynamics of aztreonam and tobramycin in hospitalized patients. Clin Ther
471		23:1231-44.
472	29.	Ioannides-Demos LL, Liolios L, Wood P, Spicer WJ, McLean AJ. 1998. Changes in MIC
473		alter responses of Pseudomonas aeruginosa to tobramycin exposure. Antimicrob Agents
474		Chemother 42:1365-9.
475	30.	Gonzalez Della Valle A, Bostrom M, Brause B, Harney C, Salvati EA. 2001. Effective
476		bactericidal activity of tobramycin and vancomycin eluted from acrylic bone cement. Acta
477		Orthop Scand 72:237-40.
478	31.	Stewart PS. 2002. Mechanisms of antibiotic resistance in bacterial biofilms. Int J Med
479		Microbiol 292:107-13.

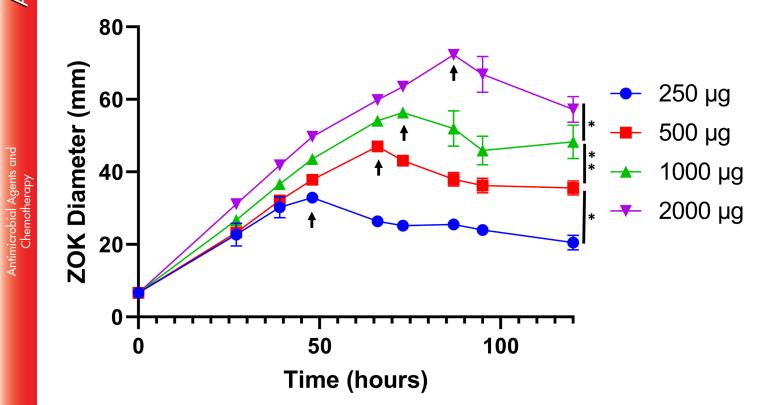
480	32.	Swearingen MC, Granger JF, Sullivan A, Stoodley P. 2016. Elution of antibiotics from
481		poly(methyl methacrylate) bone cement after extended implantation does not necessarily
401		
482		clear the infection despite susceptibility of the clinical isolates. Pathog Dis 74:ftv103.
483	33.	Dutta Sinha S, Chatterjee S, Maiti PK, Tarafdar S, Moulik SP. 2017. Evaluation of the role
484		of substrate and albumin on Pseudomonas aeruginosa biofilm morphology through FESEM
485		and FTIR studies on polymeric biomaterials. Prog Biomater 6:27-38.
486	34.	Song F, Wang H, Sauer K, Ren D. 2018. Cyclic-di-GMP and oprF Are Involved in the
487		Response of Pseudomonas aeruginosa to Substrate Material Stiffness during Attachment
488		on Polydimethylsiloxane (PDMS). Front Microbiol 9:110.
489	35.	Hoiby N, Bjarnsholt T, Moser C, Jensen PO, Kolpen M, Qvist T, Aanaes K, Pressler T,
490		Skov M, Ciofu O. 2017. Diagnosis of biofilm infections in cystic fibrosis patients. APMIS
491		125:339-343.
492	36.	Wilkinson HN, Iveson S, Catherall P, Hardman MJ. 2018. A Novel Silver Bioactive Glass
493		Elicits Antimicrobial Efficacy Against Pseudomonas aeruginosa and Staphylococcus
494		aureus in an ex Vivo Skin Wound Biofilm Model. Front Microbiol 9:1450.
495	37.	Nichols WW, Dorrington SM, Slack MP, Walmsley HL. 1988. Inhibition of tobramycin
496		diffusion by binding to alginate. Antimicrob Agents Chemother 32:518-23.

497

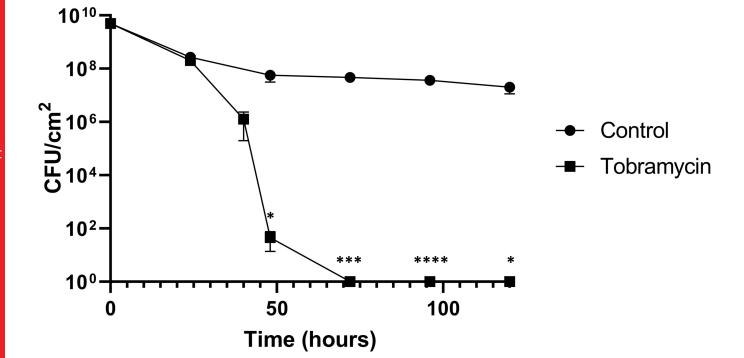
AAC



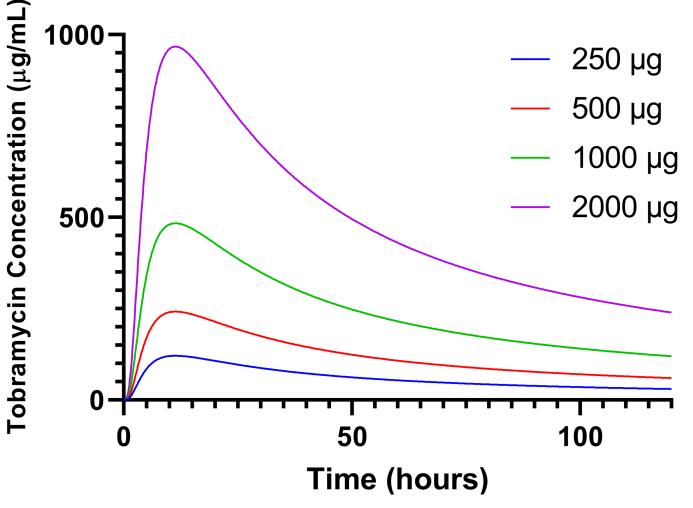




AAC



AAC





AAC

